DTU Library

Supply Inadequacy Risk Evaluation of Stand-alone Renewable Powered Heat-Electricity Energy Systems: A Data-driven Robust Approach

Cao, Yang; Wei, Wei; Chen, Laijun; Wu, Qiuwei; Mei, Shengwei

Published in:
IEEE Transactions on Industrial Informatics

Link to article, DOI:
10.1109/TII.2020.2987823

Publication date:
2021

Document Version
Peer reviewed version

Supply Inadequacy Risk Evaluation of Stand-alone Renewable Powered Heat-Electricity Energy Systems: A Data-driven Robust Approach

Yang Cao, *Student Member, IEEE,* Wei Wei, *Senior Member, IEEE,* Laijun Chen, *Member, IEEE,* Qiuwei Wu, *Senior Member, IEEE,* Shengwei Mei, *Fellow, IEEE*

***Abstract*—Integration of heat and electricity supply improves the overall energy efficiency and system operational flexibility. The renewable powered heat-electricity energy system is a promising way to set up residential energy supply facilities in remote areas beyond the reach of power system infrastructures. However, the volatility of wind and solar energy brings about the risk of supply inadequacy. This paper proposes a data-driven robust method to quantify two measures of such a risk in the stand-alone renewable powered heat-electricity energy system. The uncertainty of renewable generation is modeled through a family of ambiguous probability distributions around an empirical one based on the Wasserstein metric; then the probability of heat and electricity load shedding during a short period and related penalty cost are discussed. Through a polyhedral characterization of renewable power feasible region, the load shedding probability under the Wasserstein ambiguity set comes down to a linear program. With a piecewise linear optimal value function of the penalty cost, its expectation under the worst-case distribution in the Wasserstein ambiguity set also gives rise to a linear program. The proposed method requires moderate information on renewable generation and makes full use of available data, while sustains computational tractability. The evaluation result is robust against the inaccuracy of renewable power distributions. Case studies demonstrate the effectiveness of the proposed approach.**

***Index Terms*—data-driven robust optimization, heat-power integration, risk evaluation, renewable generation, uncertainty**

NOMENCLATURE

A. Abbreviations

COP	Coefficient of performance.
DR	Data-driven robust.
E-LSC	Expectation of load shedding cost.
ESU	Electricity storage unit.
GMM	Gaussian mixture model.
HP	Heat pump.
HEES	Heat-electricity energy system.
MCS	Monte Carlo simulation.
MP-LP	Multi-parametric linear programming.
P-LSE	Probability of load shedding event.
PDF	Probability density function.
POP	Parametric optimization.
WT	Wind turbine.
SP	Solar panel.
SoC	State-of-charge.
TSU	Thermal storage unit.

B. Parameters

COP	COP of heat pump.
Cap^R	Capacity of renewable resource.
C^P	Load shedding penalty cost for unit power.
C^H	Load shedding penalty cost for unit heat.
h_t^L	Heat loads.
p_t^L	Power loads.
P^{loss}	Permitted amount of electric load shedding.
H^{loss}	Permitted amount of heat load shedding.
η_c^E/η_d^E	Charge/discharge efficiency of the ESU.
η_c^H/η_d^H	Charge/discharge efficiency of the TSU.
μ^E	Self-discharge rate of ESU.
μ^H	Thermal dissipation rate of TSU.
T	Number of periods.

C. Decision Variables

h_t^c/h_t^d	Charge/discharge rate of TSU.
p_t^E	Electric power input from renewable resource.
h_t^{HP}	Heat output of heat pump.
h_t^{loss}	Shedding heat in period t.
p_t^{HP}	Power input of heat pump.
p_t^c/p_t^d	Charge/discharge rate of ESU.
p_t^r	Power output of renewable resource.
p_t^{loss}	Shedding power in period t.
W_t^E	Electric energy stored in ESU.
W_t^H	Thermal energy stored in TSU.

This work was supported in part by the National Natural Science Foundation of China (U1766203, 51621065, 51807101), and in part by Qinghai Science and Technology Department under Grant No. 2018-GX-A6. Corresponding author: L. Chen and S. Mei.

Y. Cao, W. Wei, L. Chen and S. Mei, are with the State Key Laboratory of Power Systems, Department of Electrical Engineering, Tsinghua University, Beijing, 100084, China (e-mails: cao-y17@mails.tsinghua.edu.cn, wei-wei04@mails.tsinghua.edu.cn, chenlaijun@tsinghua.edu.cn, meishengwei@tsinghua.edu.cn).

Q. Wu is with Department of Electrical Engineering, Technical University of Denmark, Kgs. Lyngby Denmark 2800 (e-mail: qw@elektro.dtu.dk).

I. INTRODUCTION

A. Motivation

ENERGY is the foundation of modern society. The desire for a cleaner and more sustainable society has led to a profound revolution in the energy industry. In the past decade, the share of wind and solar generation has witnessed a rapid growth worldwide [1], and there are many studies focusing on further promoting the renewable penetration [2], [3]. However, the uncertainty and volatility of renewable plants require sufficient backup capacity and storage units to maintain a balance between the generation and load in real time, causing additional costs and operational risks. In recent years, the initiative of heat-electricity integration offers a new perspective on the efficient utilization of renewable energy at the demand side [4]. Heating system possesses large thermal inertia and thermal energy storage units; thereby electric heating devices could serve as the flexible load and provide demand response to the power grid [5], [6] .

Typically, the integrated heat-electricity energy system (HEES) is supplied by power grids and district heating networks, and the cascaded utilization of different energy forms could enhance the overall efficiency of the system. Nevertheless, in remote areas beyond the reach of power system or heating system infrastructures, renewable energy is a promising resource for setting up clean and sustainable residential HEES to satisfy the local electric and thermal energy demands, because the investment on energy transportation corridor is saved, and the operation cost of renewable plants is generally very low. However, given the uncertain and volatile output of wind turbines (WT) and solar panels (SP), the stand-alone HEES may suffer from supply inadequacy without the support of power grids. To ensure safe and reliable operation, it is necessary to investigate the operational risk of stand-alone HEES.

B. Literature Review

Power system reliability/risk assessment is a traditional topic which has been studied for half a century, and relatively complete theories have been established [7]. However, with the increasing of uncertain renewable sources and the interdependence intensifying of cyber-physical system, the power system operation is facing more risks in recent years. In addition, the development of new techniques, e.g., data-driven and machine learning methods, also provides new insights to this area. Considering the coupling of information and active distribution networks, a cyber-power joint analysis method is developed in [8] to quantify the operational risks of power system via analyzing information flow and cyber contingencies of cyber systems. In [9], a hierarchical and self-adaptive data-analytics method is proposed to conduct the real-time short-term voltage stability assessment, where the the assessment accuracy and the earliness are simultaneously optimized to achieve a better evaluation performance. Based on the hybrid randomized learning systems, ref. [10] proposes a novel temporal-adaptive machine learning algorithm to assess the short-term voltage stability, and case studies on New England 39-bus system demonstrate its excellent accuracy without increased computational burden. In [11], a time-varying reliability evaluation model is introduced for wind farms, conventional and fast start-up thermal units, which could help the system operators evaluate the reliability and schedule reserve to ensure operational security in different time scales. In [12], a transmission line overload risk assessment model is developed considering the wind and load-power generation correlation. The model takes probability and severity into consideration and provides a comprehensive evaluation result for system operators. In [13], the operation risk is described as an admissibility measure brought by the uncertain wind generation. Based on such a measure, a risk-minimization model is developed to maximize and characterize the admissible region for wind power. Considering the rapid and volatile wind power variations, an intelligent framework is proposed in [14] for wind integrated power system real-time dynamic security assessment based on soft computing technologies. Through considering the wind variability, turbine forced outages and correlation of different turbines, ref. [15] establishes a wind reliability assessment model including probability and frequency distributions of wind power output, and adopts Monte Carlo simulation to demonstrate the effectiveness. In [16], a sensitivity-based decentralized framework is developed to quantify the stability indexes of power systems with uncertain renewable resources. The paradigm is conducted in a decentralized way and only uses the boundary information, which could be applied to large-scale power systems easily.

For the system equipped with storage units, system operators have more flexible resources to address operational risks. A reliability assessment model for a wind-storage system is developed in [17], and the Monte Carlo simulation is applied to calculate load reliability indexes. For the wind-power system with energy storage device, ref. [18] combines the traditional analytical and simulation methods to establish the reliability assessment model, which accelerates calculation significantly. In [19], a reliability evaluation approach based on Markov model is proposed to conduct the reliability analysis for distribution systems with mobile energy storage units, and verifies that storage units could enhance the system reliability effectively.

The aforementioned studies only focus on the risk and reliability of pure power system, however, for multi-carrier energy system involving electricity, natural gas and heat, the interdependence among energy flows brought by energy conversion facility and storage unit intensifies the difficulty of reliability/risk evaluation, calling for the development of new approaches. In [20], a reliability evaluation model is developed to calculate the supply reliability indexes in the multi-carrier energy system, so as to analyze the system benefit and sensitivity. Based on big data analytics, a critical energy function is proposed in [21] to explore small disturbance stability region, so as to evaluate the system-level stability in the Energy Internet. Considering dynamic behavior of thermal loads, a Markov-chain Monte Carlo model is introduced in [22] to analyze the mutual dependence between different energy sectors and effects on supply reliability. In [23], the supply adequacy of multi-carrier energy system is modeled and evaluated considering the interaction of energy carriers at both generation side and demand side. In [24], a combination method of reliability evaluation and system reconfiguration is proposed for the integrated energy system, which is solved via a decentralized agent communication algorithm. Ref. [25] introduces a new approach to improve the optimal load curtailment algorithm and reliability assessment algorithm for integrated power and gas system. The improved algorithm effectively enhances the computation efficiency and robust performance. In [26], a first-order reliability method is applied to estimate the failure probability in the integrated energy system considering uncertain renewable output and energy demands. The failure probability could inform system operators risky events and help maintain a safe operation. To estimate the failure probability of natural gas supply in a multi-carrier energy system, ref. [27] considers the energy network constraints and adopts the central moment method to conduct the analysis, which is superior to other traditional methods according to the comparative simulation.

The aforementioned multi-carrier systems are all connected to the power, heat or gas system infrastructures, which have relatively steady fuel supply. However, for the fully renewable powered energy system in remote areas, such an infrastructure is usually stand-alone without energy supply networks [28], [29], and the main challenge is to maintain power balancing and supply adequacy under uncertain renewable generation [30]. In [31], a hybrid optimization algorithm is developed to size a stand-alone solar-wind-hydrogen energy system considering the weather forecasting information. The hybrid algorithm combines the advantages of three algorithms (chaotic search, harmony search and simulated annealing), and has significant superiors to these individual algorithms according to case studies. Taking the renewable and load uncertainties into consideration, a hybrid algorithm based on Monte Carlo simulation method and Particle Swarm Optimization algorithm is developed in [32] to optimize the off-grid hybrid photovoltaic-wind-battery system, which could cover all generation and load possibilities and increase the system reliability. The aforementioned studies mainly focus on the planning of stand-alone renewable powered energy system, and as for the reliability assessment, ref. [33] proposes a probabilistic reliability evaluation approach and Monte Carlo simulation technique to calculate the reliability indexes for a stand-alone hybrid renewable power system in rural communities. In [34], two indices (Loss of load expectation and Expected energy not served) are proposed to investigate the reliability of PV-wind-pumped storage hydro plant system. A probabilistic upper reservoir multi-state model is developed for incorporating realistic situation using analytical technique, and is compared with traditional Monte Carlo simulation to demonstrate its advantages.

The aforementioned studies mainly focus on the stand-alone electric system, however, to the best of our knowledge, there are few studies investigating the reliability/risk evaluation of stand-alone HEES, which actually has more complicated energy flows compared with pure electric system in remote areas, thus calling for the development of new techniques. In addition, from the methodological perspective, most studies mentioned above conduct the risk evaluation based on the analytical or simulation-based methods, relying on the exact probability distribution function (PDF) of uncertain factors, which is rarely available at hand due to the lack of enough historical data. Because the probabilistic evaluation result is generally sensitive to the perturbation in the underlying PDF, using an inexact empirical distribution is likely to provide less reliable information to system operators. To address the above problems, this paper proposes a data-driven robust approach to evaluate the supply inadequacy risk of a stand-alone HEES for ensuring the system safe and reliable operation. A comprehensive tutorial on robust and distributionally robust optimization can be found in Appendix C of [35]. Nevertheless, this work encloses uncertainty quantification which is somewhat different from optimization.

C. Novelties and Contributions

In this paper, we study the short-term risk evaluation of the stand-alone fully renewable powered HEES, and the novelties and contributions are summarized as follows.

1) We propose two data-driven robust risk evaluation models. Renewable generation uncertainty is modeled by a family of PDFs which are close to the empirical distribution in the sense of Wasserstein metric. The first model provides the probability for the heat and electricity load shedding being no greater than a pre-specified value during a given period, termed as the probability of load shedding event (P-LSE) model. The second model evaluates the expected penalty cost of load shedding, termed as expectation of load shedding cost (E-LSC) model. In contrast to the traditional risk evaluation methods which rely on an exact PDF, our proposed models consider a family of inexact PDFs based upon a data-driven empirical distribution, which could provide a lower/upper bound on the desired performance with a provable guarantee on the confidence level, thus providing more reliable risk information for system operators.

2) We develop tractable reformulations for the proposed two evaluation models. The two data-driven robust risk evaluation models address the optimization over a set consisting of infinite PDFs and cannot be solved directly. For the P-LSE model, we characterize the feasible region of renewable power output via an explicit polyhedron by using the projection algorithm. For the E-LSC model, the minimum load shedding cost is expressed as a convex piecewise linear function in the renewable output based on dual theory and multi-parametric linear program (MP-LP) theory. With above techniques, the two models can be transformed into easy-to-solve linear programs via existed commercial solvers and could be applied to engineering practice easily.

The rest of the paper is organized as follows. In Section II, renewable generation is modeled by an ambiguity set consisting of all possible PDFs around the empirical one in the sense of Wasserstein metric, then two data-driven robust risk evaluation models (P-LSE and E-LSC) are introduced to identify the worst risk measures in the ambiguity set. In Section III, through a polyhedral characterization of renewable power feasible region, the P-LSE model is reformulated as a linear program; through acquiring a piecewise linear optimal value function of the penalty cost, the E-LSC model is also transformed to a linear program. In Section IV, case studies are conducted to demonstrate the effectiveness of the proposed model and method. Finally, conclusion is summarized in Section V.

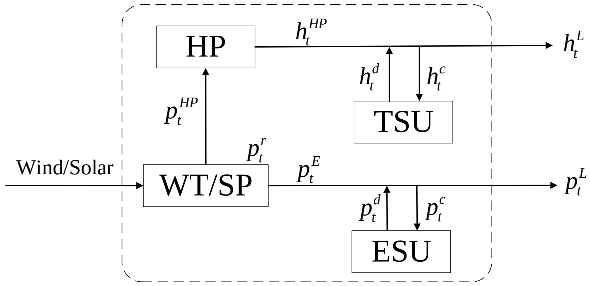

Fig. 1. Structure of the stand-alone renewable powered HEES.

II. Problem Formulation

The model of the stand-alone renewable powered HEES will be presented first; then the ambiguity set for inexact PDFs of renewable generation is given; finally, formulations of P-LSE and E-LSC models are set forth.

A. Stand-alone Renewable Powered HEES

System configuration of the stand-alone renewable powered HEES is shown in Fig. 1. The energy supply comes from wind and solar power, which is complementary across daytime and night. The energy flow is also marked in Fig.1. The WT/SP produced electricity can be used to satisfy electric demand, stored in the electricity storage unit (ESU), or consumed by heat pump (HP) to generate heat power; the HP produced thermal energy can be used to satisfy thermal demand or stored in the thermal storage unit (TSU). Here, we assume that the ESU is a battery array and the TSU is a hot water tank. Therefore, they are independent facilities and have no direct relation in energy flows. System operating constraints include:

$$p_t^r = p_t^{HP} + p_t^E \tag{1a}$$

$$h_t^{HP} = \text{COP} \cdot p_t^{HP} \tag{1b}$$

$$W_{t+1}^E = W_t^E(1-\mu^E) + (p_t^c \eta_c^E - p_t^d/\eta_d^E)\Delta t \tag{1c}$$

$$W_{t+1}^H = W_t^H(1-\mu^H) + (h_t^c \eta_c^H - h_t^d/\eta_d^H)\Delta t \tag{1d}$$

$$p_t^E + p_t^d - p_t^c \ge p_t^L \tag{1e}$$

$$h_t^{HP} + h_t^d - h_t^c \ge h_t^L \tag{1f}$$

$$\text{Cons-BND} \tag{1g}$$

where equation (1a) describes the energy allocation from renewable sources; equation (1b) describes the thermal energy produced by HP depending on the input electric power; equations (1c) and (1d) are the state-of-charge (SoC) dynamics of ESU and TSU; equations (1e) and (1f) depict the electric and thermal power balance. We do not impose a strict equality between supply and load, which means that the excessive renewable power will be curtailed. Cons-BND collects all variable lower and upper bound constraints, reflecting the physical capacity of system components.

B. Constructing the Ambiguity Set

The uncertainty of renewable generation will significantly influence the load supply adequacy. Therefore, it is important to investigate the risk of load shedding caused by the uncertainty and volatility of renewable power. We consider the problem in the future two or three hours when renewable generation is predicted to drop rapidly. Equipment failure is ignored in such a short time period. Since the system is small and controlled by a central operator, the heat and electricity loads are also deterministic. So the only uncertain factor is the renewable power output.

Let $\boldsymbol{\xi}$ denotes the uncertain renewable power output, it is essential to acquire the probability distribution function (PDF) of random variable $\boldsymbol{\xi}$ based on the historical data. The empirical distribution P_0 could be constructed as follows.

$$\mathrm{P}_0 = \frac{1}{N}\sum_{i=1}^{N} \delta_{\boldsymbol{\xi}_i^0}$$

where P_0 consists of N independent samples $\{\boldsymbol{\xi}_1^0, \boldsymbol{\xi}_2^0, ..., \boldsymbol{\xi}_N^0\}$, and each of them has a probability of $1/N$. $\delta_{\boldsymbol{\xi}_i^0}$ denotes Dirac distribution concentrating unit mass at $\boldsymbol{\xi}_i^0$.

However, without enough historical data, the empirical distribution P_0 is usually inaccurate. As a result, we resort to the construction of an ambiguity set containing all possible PDFs that are close to the empirical distribution P_0. This entails a definition of the distance between two PDFs. In this paper, the Wasserstein metric is adopted to quantify such a distance, which is defined as follows [36].

$$\begin{aligned} D_W(\mathrm{P},\mathrm{P}_0) = \inf \quad & \int_{\Xi^{\mathrm{m}}} \left\|\boldsymbol{\xi} - \boldsymbol{\xi}^0\right\|_p \Pi(\mathrm{d}\boldsymbol{\xi}, \mathrm{d}\boldsymbol{\xi}^0) \\ \text{s.t.} \quad & \Pi \text{ is a joint distribution of } \boldsymbol{\xi} \\ & \text{and } \boldsymbol{\xi}^0 \text{ with marginals P and } \mathrm{P}_0 \end{aligned} \tag{2}$$

where $\|\cdot\|_p$ represents the p-norm on $\mathbb{R}^m$. The definition of Wasserstein metric could be viewed as the optimal transportation plan which moves a mass distribution P to another distribution P_0 with minimum transportation cost. Based on such a definition, the Wasserstein metric for two discrete distributions can be expressed by

$$\begin{aligned} D_W(\mathrm{P},\mathrm{P}_0) = \inf_{\pi \ge 0} \quad & \sum_i \sum_j \pi_{ij} \left\|\boldsymbol{\xi}_j - \boldsymbol{\xi}_i^0\right\|_p \\ \text{s.t.} \quad & \sum\nolimits_j \pi_{ij} = p_i^0, \ \forall i \\ & \sum\nolimits_i \pi_{ij} = p_j, \ \forall j \end{aligned} \tag{3}$$

where p_i^0 and p_j denote the probability of representative scenario $\boldsymbol{\xi}_i^0$ and $\boldsymbol{\xi}_j$.

With the Wasserstein metric, the ambiguity set could be constructed as the following form:

$$\mathbb{P} = \{P | D_W(\mathrm{P},\mathrm{P}_0) \le d_w\} \tag{4}$$

where d_w is a critical parameter determining the size of the ambiguity set $\mathbb{P}$. Clearly, set $\mathbb{P}$ grows larger with the increasing value of d_w, implying that more PDFs are taken into account. On the other hand, the size of set $\mathbb{P}$ should depend on the amount of historical data. When more data is available, we will be more confident on the accuracy of the empirical distribution P_0. Suppose we have N samples at hand, then d_w could be chosen as [37]:

$$d_w = \sqrt{\frac{1}{N}\ln(\frac{1}{1-\beta})} \tag{5}$$

where β denotes the confidence level, which means that if we choose d_w according to (5), then the probability for the actual PDF $\mathrm{P} \in \mathbb{P}$ is no less than β. This parameter reflects the system operators' attitudes towards risks.

C. Estimating the Probability of Load Shedding Events

In system operation, it is important to estimate the probability of load shedding events (P-LSE) due to the uncertainty and volatility of renewable power output. The system operation challenges brought by such kind of uncertainty may vary across several hours, and the number of periods T should be specified first.

To define a load shedding event, the heat and power balance constraints in (1e) and (1f) are revamped as

$$\begin{aligned} p_t^E + p_t^d - p_t^c + p_t^{loss} \geq p_t^L \\ h_t^{HP} + h_t^d - h_t^c + h_t^{loss} \geq h_t^L \\ \sum\nolimits_{t=1}^T p_t^{loss} \leq P^{loss}, p_t^{loss} \geq 0 \\ \sum\nolimits_{t=1}^T h_t^{loss} \leq H^{loss}, h_t^{loss} \geq 0 \end{aligned} \tag{6}$$

where P^{loss} and H^{loss} denote the amounts of acceptable electricity and heat load shedding; if they are set to zero, load shedding is not allowed; p_t^{loss} and h_t^{loss} represent the amounts of electricity and heat load shedding in period t.

Let vector $\boldsymbol{\xi}$ collects the renewable output $p_t^r, \forall t$, and vector $\boldsymbol{x}$ encapsulates all the other decision variables in constraints (1a)-(1g) together with p_t^{loss} and h_t^{loss}; P^{loss} and H^{loss} are given constants. The operation constraints considering load shedding consist of (1a)-(1d), (1g) and (6), which could be written in a compact matrix form as

$$\boldsymbol{A\xi} + \boldsymbol{Bx} \leq \boldsymbol{c} \tag{7}$$

where matrices $\boldsymbol{A}$, $\boldsymbol{B}$, and vector $\boldsymbol{c}$ are constants corresponding to the coefficients in (1a)-(1d), (1g) and (6).

Define the feasible set W of renewable output as follows

$$W = \{\boldsymbol{\xi} \in \mathbb{R}^m | \exists \boldsymbol{x} : \boldsymbol{A\xi} + \boldsymbol{Bx} \leq \boldsymbol{c} \quad \text{is met}\} \tag{8}$$

where m is the dimension of $\boldsymbol{\xi}$. Set W is the projection of polyhedron (7) onto the $\boldsymbol{\xi}$-subspace. We will shed light on how to compute W in the next section. According to this definition, the minimal amount of load shedding will not exceed P^{loss} and H^{loss} as long as $\boldsymbol{\xi} \in W$. So a load shedding event is triggered by

$$\boldsymbol{\xi} \notin W$$

On this account, W provides a convenient tool for determining whether a load shedding event will happen. Please keep in mind that the load shedding event depends on P^{loss} and H^{loss}, and different values define different load shedding events.

To access the worst probability of a load shedding event under ambiguous PDFs of renewable output restricted in the ambiguity set (4), the data-driven robust P-LSE problem is cast as follows.

$$\sup_{\mathrm{P} \in \mathbb{P}} \Pr\{\boldsymbol{\xi} \notin W\} \tag{9}$$

where $\Pr$ indicates the probability evaluated under some PDF P; $\mathbb{P}$ is the ambiguity set (4) containing all possible PDFs.

Problem (9) aims to identify the load shedding probability with respect to the worst-case PDF in $\mathbb{P}$, and actually provides system operators the probability upper bound for the amount of load shedding exceeding threshold values P^{loss} and H^{loss}, which means that no matter how the actual PDF varies in practice, the system risk will never exceed the estimated results of problem (9). Such information is very useful for system operation which usually requires a high reliability. It is worth mentioning that the ambiguity set $\mathbb{P}$ is associated with the parameter d_w in (5), which is influenced by available historical data N and the operator's risk preference β. If more data is at hand, the estimated upper bound would be less conservative, implying the method takes full advantage of historical data.

D. Estimating the Expectation of Load Shedding Cost

If load shedding incurs economic losses, it is also important to have certain knowledge about the cost associated with load shedding. Due to the uncertainty and volatility of renewable power output, we tend to estimate the expectation of load shedding cost (E-LSC). Firstly, given renewable output $\boldsymbol{\xi}$ as a parameter, the deterministic cost could be expressed as the following minimization problem.

$$L(\boldsymbol{\xi}) = \min \quad C^P \sum_{t=1}^T p_t^{loss} + C^H \sum_{t=1}^T h_t^{loss} \tag{10a}$$

$$\text{s.t.} \quad \text{constraints (1a)-(1d) and (1g)} \tag{10b}$$

$$p_t^E + p_t^d - p_t^c + p_t^{loss} \geq p_t^L \tag{10c}$$

$$h_t^{HP} + h_t^d - h_t^c + h_t^{loss} \geq h_t^L \tag{10d}$$

$$p_t^{loss} \geq 0, h_t^{loss} \geq 0 \tag{10e}$$

where C^P and C^H are the cost of shedding one unit of electric and heat load. In fact, the objective function can consider any convex cost function which can be approximated by piecewise linear functions without jeopardizing the linearity of (10). For example, the cost of casting off electricity load is a convex function $f_t(p_t^{loss})$; we can divide the concerned interval of p_t^{loss} into several segments with break points $p_{t1}^{loss}, \cdots, p_{tK}^{loss}$, and their corresponding function values are $f_{t1}, \cdots, f_{tK}$. Associate each pair (p_{tk}^{loss}, f_{tk}) with a weight coefficient variable λ_{tk} satisfying $\lambda_{tk} \geq 0$, $\sum_k \lambda_{tk} = 1$, then the nonlinear cost function can be replaced with $f_t(p_t^{loss}) = \sum_k \lambda_{tk} f_{tk}$ which is linear in λ_{tk}, and linear equality $p_t^{loss} = \sum_k \lambda_{tk} p_{tk}^{loss}$ is included in the constraints.

To access the worst expectation of load shedding cost under ambiguous PDFs of renewable output restricted in the ambiguity set (4), the data-driven robust E-LSC problem is cast as follows.

$$\sup_{\mathrm{P} \in \mathbb{P}} E_P[L(\boldsymbol{\xi})] \tag{11}$$

where $E_P[\cdot]$ denotes the expectation operator with respect to some PDF P; $L(\boldsymbol{\xi})$ is the minimal load shedding cost associated with $\boldsymbol{\xi}$. Problem (11) aims to identify the expectation cost under the worst-case PDF in $\mathbb{P}$, which offers an upper bound of economic loss caused by load shedding under renewable generation uncertainty. Similar to problem (9), such a bound could also provide more reliable information for system operators, and is also affected by parameter d_w and thus data availability.

III. Solution Strategy

Problems (9) and (11) cannot be solved directly because they address the optimization over the ambiguity set (4) consisting of infinite PDFs. In this section, tractable reformulations of P-LSE and E-LSC models are developed.

A. Reformulation of P-LSE Model

In P-LSE problem (9), the difficulty rests on the fact that the feasible region W of uncertain variable $\boldsymbol{\xi}$ is not explicitly expressed in $\boldsymbol{\xi}$. Therefore, we need to project polyhedron (7) onto the $\boldsymbol{\xi}$-subspace, which is defined as polyhedron (8). It is proven in [38] that polyhedron (8) has the following equivalent form:

$$W = \{\boldsymbol{\xi} \in \mathbb{R}^m \mid \boldsymbol{u}^\top \boldsymbol{A}\boldsymbol{\xi} \geq \boldsymbol{u}^\top \boldsymbol{C}, \forall \boldsymbol{u} \in \text{vert}(U)\} \tag{12}$$

where $U = \{\boldsymbol{u} \mid \boldsymbol{B}^\top \boldsymbol{u} = 0, -1 \leq \boldsymbol{u} \leq 0\}$ is a bounded polyhedron, and vert(U) denotes all vertices of U.

In fact, most elements of vert(U) will generate a redundant inequality, and there is no need to enumerate all vertices of U to construct the expression of W. We use the algorithm developed in [38] to perform polyhedral projection, and obtain the following formula.

$$W = \{\boldsymbol{\xi} \in \mathbb{R}^m | \boldsymbol{D}\boldsymbol{\xi} \leq \boldsymbol{f}\} \tag{13}$$

where constant matrix $\boldsymbol{D}$ and vector $\boldsymbol{f}$ are the output of the projection algorithm. In this way, the non-explicit polyhedron (8) has been equivalently transformed to the explicit polyhedral form (13).

Given the explicit polyhedral form of W, the P-LSE problem (9) gives rise to the uncertainty quantification problem discussed in [39]. Since we use the Wasserstein metric based ambiguity set, the P-LSE problem (9) could be reformulated as the following optimization problem [39].

$$\begin{aligned}
\min \quad & 1 + \gamma d_w - \frac{1}{N}\sum_{n=1}^{N} \sigma_n && \text{(14a)}\\
\text{s.t.} \quad & \boldsymbol{\sigma} \in \mathbb{R}^N, \gamma \in \mathbb{R}_+, \boldsymbol{\tau} \in \mathbb{R}_+^{N \times I} && \text{(14b)}\\
& \sigma_n \leq 1, \quad \forall n \leq N && \text{(14c)}\\
& \sigma_n + \tau_{ni}\boldsymbol{D}_i\boldsymbol{\xi}_n \leq \tau_{ni} f_i, \quad \forall n \leq N, \forall i \leq I && \text{(14d)}\\
& \|\tau_{ni}\boldsymbol{D}_i\|_q \leq \gamma, \quad \forall n \leq N, \forall i \leq I && \text{(14e)}
\end{aligned}$$

where $\boldsymbol{\sigma}, \gamma$ and $\boldsymbol{\tau}$ are all auxiliary variables; $\boldsymbol{D}_i$ and f_i denote the i-th row of matrix $\boldsymbol{D}$ and vector $\boldsymbol{f}$; $\|\cdot\|_q$ is the dual norm of $\|\cdot\|_p$ which appeared in the Wasserstein metric (3), where p and q satisfy $p^{-1} + q^{-1} = 1$.

The objective function and constraints in problem (14) are linear, except for (14e). Nevertheless, it actually gives rise to a linear inequality when $p = 1$ or $p = \infty$ and a second-order cone one when $p = 2$. In this paper, we choose $p = \infty$, $q = 1$ and thus constraint (14e) becomes the following linear inequality.

$$\tau_{ni} \sum_j |D_{ij}| \leq \gamma \tag{15}$$

where D_{ij} denotes the element of $\boldsymbol{D}$.

Finally, the P-LSE problem (9) comes down to a linear program, which could be solved efficiently.

B. Reformulation of E-LSC Model

In E-LSC problem (11), the difficulty rests on the fact that $L(\boldsymbol{\xi})$ is defined by an optimization problem, while we need an analytical expression of the optimal value function $L(\boldsymbol{\xi})$ in variable $\boldsymbol{\xi}$. To be distinguishable with P-LSE, let $\boldsymbol{y}$ be the decision variables in linear program (10), and the definition (10) of $L(\boldsymbol{\xi})$ could be rewritten as a compact matrix form.

$$L(\boldsymbol{\xi}) = \left\{ \min_{\boldsymbol{y}} \boldsymbol{c}^\top \boldsymbol{y} \;\middle|\; \boldsymbol{G}\boldsymbol{y} \geq \boldsymbol{H}\boldsymbol{\xi} + \boldsymbol{h} \right\} \tag{16}$$

According to the dual theory of linear program, the dual problem of (16) is

$$\begin{aligned}
L(\boldsymbol{\xi}) &= \left\{ \max_{\boldsymbol{\theta}} (\boldsymbol{H}\boldsymbol{\xi} + \boldsymbol{h})^\top \boldsymbol{\theta} \;\middle|\; \boldsymbol{G}^\top \boldsymbol{\theta} = \boldsymbol{c}, \boldsymbol{\theta} \geq 0 \right\} \\
&= \max_{k \leq K} \left\{ v_k^\top \boldsymbol{H}\boldsymbol{\xi} + v_k^\top \boldsymbol{h} \right\}
\end{aligned} \tag{17}$$

where $\boldsymbol{\theta}$ stands for the dual variable; v_k, $k = 1, \cdots, K$ are the extreme points of $V = \{\boldsymbol{\theta} \mid \boldsymbol{G}^\top \boldsymbol{\theta} = \boldsymbol{c}, \boldsymbol{\theta} \geq 0\}$. As strong duality always holds for linear programs, the optimal value of (17) is equal to $L(\boldsymbol{\xi})$.

In (17), $L(\boldsymbol{\xi})$ is finally expressed as the maximum of a family of linear functions in $\boldsymbol{\xi}$, and thus is a convex function. However, we do not need to enumerate all the vertices to construct the expression of $L(\boldsymbol{\xi})$, because most of them produce redundant functions that are never an effective part of $L(\boldsymbol{\xi})$. As a result, we resort to the multi-parameter program solver POP (Parametric Optimization) toolbox [40], to retrieve the piecewise linear functions in (17). To be specific, we use POP to solve problem (10) with $\boldsymbol{\xi}$ being the parameter. The solver returns a result in form of

$$L(\boldsymbol{\xi}) = \begin{cases} \boldsymbol{a}_1^\top \boldsymbol{\xi} + \boldsymbol{b}_1 & \boldsymbol{\xi} \in \Xi_1 \\ \quad\vdots & \\ \boldsymbol{a}_K^\top \boldsymbol{\xi} + \boldsymbol{b}_K & \boldsymbol{\xi} \in \Xi_K \end{cases} \tag{18}$$

where $\Xi_1, \cdots, \Xi_K$ are critical regions on which each linear function is in use. In the general form (18), a piecewise linear function can be either convex or non-convex. Nevertheless, the piecewise linear maximization form of $L(\boldsymbol{\xi})$ in (17) has already demonstrated its convexity, so (17) and (18) are indeed equivalent. Therefore, the analytical expression of $L(\boldsymbol{\xi})$ is

$$L(\boldsymbol{\xi}) = \max_{1 \leq k \leq K} (\boldsymbol{a}_k^\top \boldsymbol{\xi} + \boldsymbol{b}_k) \tag{19}$$

without the need of critical regions, where $\boldsymbol{a}_k^\top = v_k^\top \boldsymbol{H}$, and $\boldsymbol{b}_k = v_k^\top \boldsymbol{h}$.

We assume that the support set of $\boldsymbol{\xi}$ is

$$\Phi = \left\{ \boldsymbol{\xi} \;\middle|\; 0 \leq p_t^r \leq \text{Cap}^R \right\} \tag{20}$$

whose compact matrix form is $\Phi = \{\boldsymbol{\xi} | \boldsymbol{P}\boldsymbol{\xi} \le \boldsymbol{r}\}$. The support set (20) contains all possible values of $\boldsymbol{\xi}$, and implies that the renewable power can neither become negative nor exceed the installed capacity. Unlike the feasible region W in equation (8), support set (20) is independent of system operating point.

Once $L(\boldsymbol{\xi})$ is represented by the form of (19), the E-LSC problem (11) gives rise to the following problem [36].

$$\min \quad \lambda d_w + \frac{1}{N}\sum_{n=1}^{N} s_n \tag{21a}$$

$$\text{s.t.} \quad \eta_{nk} \ge 0, \ \forall n \le N, \forall k \le K \tag{21b}$$

$$\boldsymbol{b}_k + \boldsymbol{a}_k^\top \boldsymbol{\xi}_n + \eta_{nk}^\top (\boldsymbol{r} - \boldsymbol{P}\boldsymbol{\xi}_n) \le s_n, \quad \forall n \le N, \forall k \le K \tag{21c}$$

$$\|\boldsymbol{P}^\top \eta_{nk} - \boldsymbol{a}_k\|_q \le \lambda, \ \forall n \le N, \forall k \le K \tag{21d}$$

where λ, s_n and η_{nk} are all auxiliary variables.

The objective function and constraints in problem (21) are linear, except for constraint (21d). Here we also choose $p = \infty, q = 1$ and (21d) becomes:

$$\sum_{m=1}^{M} |(\boldsymbol{P}^\top \eta_{nk} - \boldsymbol{a}_k)_m| \le \lambda \tag{22}$$

where M denotes the dimension of $\boldsymbol{\xi}$; $(\boldsymbol{P}^\top \eta_{nk} - \boldsymbol{a}_k)_m$ denotes the m-th element of column vector $\boldsymbol{P}^\top \eta_{nk} - \boldsymbol{a}_k$. To further linearize the absolute value function in (22), define

$$\begin{aligned} Au_m^1 &= \frac{|(\boldsymbol{P}^\top \eta_{nk} - \boldsymbol{a}_k)_m| + (\boldsymbol{P}^\top \eta_{nk} - \boldsymbol{a}_k)_m}{2} \\ Au_m^2 &= \frac{|(\boldsymbol{P}^\top \eta_{nk} - \boldsymbol{a}_k)_m| - (\boldsymbol{P}^\top \eta_{nk} - \boldsymbol{a}_k)_m}{2} \end{aligned} \tag{23}$$

Then equation (22) could be rewritten as linear constraints.

$$\begin{aligned} &(\boldsymbol{P}^\top \eta_{nk} - \boldsymbol{a}_k)_m = Au_m^1 - Au_m^2 \\ &\sum_{m=1}^{M} (Au_m^1 + Au_m^2) \le \lambda \\ &Au_m^1 \ge 0, Au_m^2 \ge 0 \end{aligned} \tag{24}$$

Finally, the E-LSC problem (11) is transformed to a linear program, which could be solved efficiently.

IV. Case Studies

A test system is used to validate the performance of the proposed model. Parameters of system components are shown in Table I. For the energy storage units, the last column "Capacity" represents the maximum stored energy and maximum charging/discharging power. In normal conditions, load shedding is not allowed. Particularly, we consider the situation in which the renewable power is predicted to be dropping fast (a downward ramping event), which is the main source of load shedding. We focus on evaluating the risk for the future two periods. The electric and heat load values are assumed to be in the intervals [2.7, 3.0] MW and [2.0, 1.8] MW, respectively. The load shedding cost coefficients are $C^P = 1000$\$/MWh and $C^H = 300$\$/MWh, respectively. The predicted wind and solar power output is assumed to be [5, 2.5] MW and [2, 2.5] MW, thus the total renewable output is [7, 5] MW, which is a downward ramping event. Real renewable generation data from Qinghai Province in China are adopted, and we generate 1000 samples for the renewable forecasting errors as the historical data. In addition, the confidence level β is assumed to be 95% for constructing the ambiguity set (4), and $d_w = 0.0547$ according to (5). All experiments are conducted on a laptop with i5-7300HQ CPU and 8G memory. The optimization models are established by YALMIP interface in MATLAB 2018a environment; linear programs are solved by CPLEX 12.8.

TABLE I
Equipment Data

	Parameters	Capacity
WT	\	6 MW
SP	\	4 MW
HP	COP = 3	5 MW
ESU	$\eta_c^E = 0.95, \eta_d^E = 0.95, \mu^E = 0.02$	5 MWh/1.5 MW
TSU	$\eta_c^H = 0.90, \eta_d^H = 0.90, \mu^H = 0.05$	5 MWh/1.5 MW

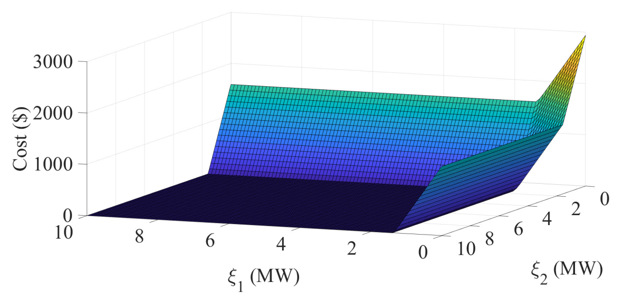

Fig. 2. Load Shedding Cost in Polyhedral Expression.

For the P-LSE problem (9), P^{loss} and H^{loss} are set to zero in the benchmark case. For the E-LSC problem (11), the convex piecewise linear representation of $L(\boldsymbol{\xi})$ is a key step. Fig. 2 plots the surface of $L(\boldsymbol{\xi})$ calculated by POP toolbox, showing its convexity.

The proposed data-driven robust (DR) method is compared with the Monte Carlo simulation (MCS) method proposed in [32]. In the process of MCS method, we first estimate the PDF for uncertain renewable generation based on the historical data at hand. Here, in order to increase the estimation accuracy, we adopt the Gaussian mixture model (GMM) to estimate the PDF. GMM is a mixture of several Gaussian distributions and could characterize the uncertainties obeying arbitrary distributions, which has been widely used to fit probability distributions of renewable power recently [41], [42]. Then we generate 100,000 samples based on the estimated PDF and calculate the two risk measures (P-LSE and E-LSC) using Monte Carlo simulation. The P-LSE and E-LSC provided by the proposed DR and MCS methods are listed in Table II. Clearly, results offered by the DR method is more conservative than those offered by the MCS method, because the latter only accounts for a particular distribution while the former considers all candidate distributions in the ambiguity set (4).

TABLE II
RISK EVALUATION RESULTS

		DR	MCS
P-LSE	Probability	19.02%	9.21%
	CPU Time (s)	6.57	34.23
E-LSC	Cost ($)	128.44	29.32
	CPU Time (s)	7.79	36.42

From the system operator's point of view, the DR method is more trustworthy because no matter how the actual PDF varies in practice, the actual P-LSE and E-LSC are no greater than the evaluated values. However, the MCS method possesses no such a guarantee because the distribution of renewable generation must be specified to perform scenario generation. The computation time of the DR method is about 7 seconds, which is much shorter than that of the MCS method, because the GMM estimation process in latter one is time-consuming. This implies that the proposed DR method could meet the requirement of online application better.

A main advantage of the proposed DR method is that its evaluation results are insensitive and robust to PDF perturbations in practice, and we conduct an experiment to verify the robustness. We generate a series of PDFs which have different Wasserstein distances d_p^0 with the empirical PDF derived from the original historical data, which imitates the PDF perturbations in practice. Next, we calculate the two actual risk measures (P-LSE and E-LSC) under these different PDFs. The Wasserstein distances d_p^0 are calculated according to equation (3) and the test results are shown in Table III. Compared with the evaluation results in Table II, it is obvious that when the actual PDF varies in practice, the actual risk measures will exceed the evaluation results of MCS method, which means that it could not provide reliable risk information for system operation when the designated PDF is inaccurate. In contrast, as for the proposed DR method, the actual risk measures are always smaller than our evaluation results until d_p^0 reaches 0.07, which is larger than the adopted parameter d_w=0.0547. This experiment demonstrates the distributional robustness of the proposed DR method, which is able to address the PDF perturbations in practice and meet the system operation requirement with higher reliability.

Parameter d_w determines the size of ambiguity set (4) and influences the model performance. According to equation (5), d_w gets smaller with the increase of N and the decrease of β. A larger d_w leads to a more conservative evaluation result due to the lack of historical data or a more prudent attitude towards risks. The impact of the values of N and β on the evaluation results are exhibited in Table IV. It is observed that the estimated probabilities and costs all decrease with a smaller value of d_w. In summary, for system operators, it is vital to collect as many historical samples as possible to reduce the conservativeness, and they also need to make a trade-off between conservativeness and robustness when choosing the confidence level β.

TABLE III
RISK MEASURES WITH DIFFERENT PDFS

d_p^0	P-LSE	E-LSC
0.01	12.65%	58.23
0.02	13.92%	74.43
0.03	15.35%	88.50
0.04	16.55%	101.06
0.05	17.63%	112.29
0.06	18.64%	122.79
0.07	19.59%	132.82
0.08	20.48%	141.78

TABLE IV
RISK EVALUATION RESULTS WITH DIFFERENT N AND β

Pro & Cost($) \ β / N	0.99	0.95	0.90
100	34.82% & 271.52	31.33% & 231.85	29.47% & 210.58
200	28.37% & 215.13	25.51% & 186.88	23.98% & 171.81
500	22.11% & 162.54	19.92% & 143.91	18.75% & 133.72
1000	20.72% & 143.39	19.02% & 128.44	18.09% & 120.22
2000	18.51% & 119.60	17.17% & 107.69	16.44% & 101.21
5000	16.07% & 97.93	15.01% & 88.70	14.41% & 83.71

In the benchmark case of P-LSE problem (9), load shedding is not allowed in the construction of feasible region W. It is useful to investigate the situation in which load shedding is permitted to some extent. This can be implemented by assigning positive values to parameters P^{loss} and H^{loss} in equation (6); then the corresponding feasible region W would become larger and thus affects the probability of the load shedding event associated with P^{loss} and H^{loss}. In our tests, we change the values of P^{loss} and H^{loss} from 0 to 2 MW, and results are shown in Fig. 3. Apparently, the estimated probabilities decrease with the growth of P^{loss} and H^{loss}, and P^{loss} has a more evident impact than H^{loss}, as the surface changes quickly along the axis of P^{loss}. This is because the COP of the heat pump is 3, i.e., 1 MWh of electric energy can be converted into 3 MWh thermal energy. Therefore, the probability is mainly affected by the change of P^{loss}, implying that the investment on power equipment, e.g., ESU, will be more effective in reducing the risk of inadequacy.

Finally, we examine the role of ESU and TSU in reducing the probability of load shedding and related penalty cost. In our tests, we change the capacities of ESU and TSU by multiplying their values with a scalar ζ, and results are given in Table V. When the capacities of energy storage units become larger, the system gains higher flexibility to mitigate the uncertainty of renewable power output, and both P-LSE and E-LSC decrease. From these results, we could conclude

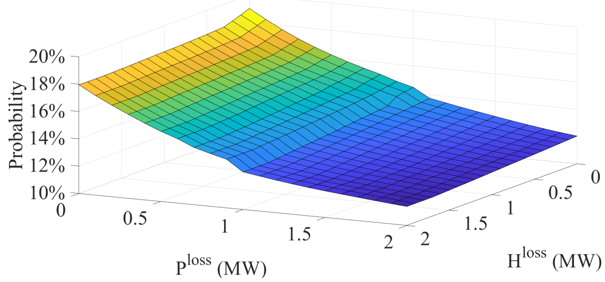

Fig. 3. Load Shedding Probabilities with Different Limitations.

TABLE V
RISK EVALUATION RESULTS WITH DIFFERENT ENERGY STORAGE CAPACITY

ζ	Probability	Cost ($)
0.4	32.36%	311.52
0.6	27.40%	236.09
0.8	22.58%	177.03
1.0	19.02%	128.44
1.2	16.46%	87.60
1.4	14.47%	61.88
1.6	13.07%	38.61

that the investment in energy storage units has a positive impact on improving the reliability. If the investment cost is taken into account, two phenomena should be considered when making a decision on capacity planning. First, although ESU has a more decisive impact on system flexibility than the TSU, the unit capacity cost of ESU is generally higher than that of TSU. Second, according to Table V, the marginal benefit, in terms of both P-LSE and E-LSC, shrinks with the growing size of storage units.

V. CONCLUSION

This paper proposes a data-driven robust method to evaluate the supply inadequacy risk of stand-alone fully renewable powered heat-electricity energy systems, including the probability of load shedding event and the expectation of load shedding cost. Compared with traditional risk evaluation methods, the proposed method shows two appealing advantages: First, the inexact distribution of renewable generation is modeled by a Wasserstein metric based ambiguity set, thus the proposed model does not rely on a specific empirical distribution, which makes the evaluation results to be insensitive and robust to PDF perturbations in practice; Second, the proposed method allows tractable reformulations as linear programs, which has relatively high computational efficiency and could be applied to online operation easily. In addition, the proposed method could reveal the quantitative dependence between the risk measures and system operation parameters (e.g., allowable load shedding amounts) and configuration parameters (e.g., capacity of energy storage units), and thus could provide useful information to the eligible decision maker for preparing better planning and operation strategies under renewable generation uncertainty.

REFERENCES

[1] M. H. Rehmani, M. Reisslein, A. Rachedi, M. Erol-Kantarci, and M. Radenkovic, "Integrating renewable energy resources into the smart grid: Recent developments in information and communication technologies," *IEEE Trans. Industrial Informatics*, vol. 14, no. 7, pp. 2814–2825, Mar. 2018.

[2] C. Dang, X. Wang, X. Wang, F. Li, and B. Zhou, "DG planning incorporating demand flexibility to promote renewable integration," *IET Gener. Transm. Distrib.*, vol. 12, no. 20, pp. 4419–4425, Nov. 2018.

[3] S. Motie, F. Keynia, M. R. Ranjbar, and A. Maleki, "Generation expansion planning by considering energy-efficiency programs in a competitive environment," *Int. J. Electr. Power Energy Syst.*, vol. 80, pp. 109–118, 2016.

[4] A. Shabanpour-Haghighi and A. R. Seifi, "Energy flow optimization in multicarrier systems," *IEEE Trans. Industrial Informatics*, vol. 11, no. 5, pp. 1067–1077, Jul. 2015.

[5] N. Liu, L. He, X. Yu, and L. Ma, "Multiparty energy management for grid-connected microgrids with heat-and electricity-coupled demand response," *IEEE Trans. Industrial Informatics*, vol. 14, no. 5, pp. 1887–1897, Sep. 2017.

[6] H. R. Massrur, T. Niknam, and M. Fotuhi-Firuzabad, "Investigation of carrier demand response uncertainty on energy flow of renewable-based integrated electricity–gas–heat systems," *IEEE Trans. Industrial Informatics*, vol. 14, no. 11, pp. 5133–5142, Jan. 2018.

[7] W. Li, *Risk Assessment of Power Systems: Models, Methods, and Applications*. John Wiley & Sons, 2014.

[8] G. Cao, W. Gu, P. Li, W. Sheng, K. Liu, L. Sun, Z. Cao, and J. Pan, "Operational risk evaluation of active distribution networks considering cyber contingencies," *IEEE Trans. Industrial Informatics*, 2019.

[9] Y. Zhang, Y. Xu, Z. Y. Dong, and R. Zhang, "A hierarchical self-adaptive data-analytics method for real-time power system short-term voltage stability assessment," *IEEE Trans. Industrial Informatics*, vol. 15, no. 1, pp. 74–84, Jan. 2019.

[10] C. Ren, Y. Xu, Y. Zhang, and R. Zhang, "A hybrid randomized learning system for temporal-adaptive voltage stability assessment of power systems," *IEEE Trans. Industrial Informatics*, 2019.

[11] Y. Ding, C. Singh, L. Goel, and et al., "Short-term and medium-term reliability evaluation for power systems with high penetration of wind power," *IEEE Trans. Sustain. Energy*, vol. 5, no. 3, pp. 896–906, Jul. 2014.

[12] X. Li, X. Zhang, L. Wu, and et al., "Transmission line overload risk assessment for power systems with wind and load-power generation correlation," *IEEE Trans. Smart Grid*, vol. 6, no. 3, pp. 1233–1242, May 2015.

[13] C. Wang, F. Liu, J. Wang, and et al., "Risk-based admissibility assessment of wind generation integrated into a bulk power system," *IEEE Trans. Sustain. Energy*, vol. 7, no. 1, pp. 325–336, Jan. 2015.

[14] Y. Xu, Z. Y. Dong, Z. Xu, K. Meng, and K. P. Wong, "An intelligent dynamic security assessment framework for power systems with wind power," *IEEE Trans. Industrial Informatics*, vol. 8, no. 4, pp. 995–1003, Jun. 2012.

[15] S. Sulaeman, M. Benidris, J. Mitra, and C. Singh, "A wind farm reliability model considering both wind variability and turbine forced outages," *IEEE Trans. Sustain. Energy*, vol. 8, no. 2, pp. 629–637, Apr. 2016.

[16] M. Z. Jahromi, M. Tajdinian, J. Zhao, P. Dehghanian, M. Allahbakhsi, and A. R. Seifi, "Enhanced sensitivity-based decentralised framework for real-time transient stability assessment in bulk power grids with renewable energy resources," *IET Gener. Transm. Distrib.*, vol. 14, no. 4, pp. 665–674, Feb. 2020.

[17] I. Hussein and M. AlMuhaini, "Reliability assessment of integrated wind-storage systems using monte carlo simulation," in *2016 13th International Multi-Conference on Systems, Signals & Devices (SSD)*. IEEE, 2016, pp. 709–713.

[18] F. Bhuiyan and A. Yazdani, "Reliability assessment of a wind-power system with integrated energy storage," *IET Renew. Power Gener.*, vol. 4, no. 3, pp. 211–220, May 2010.

[19] Y. Chen, Y. Zheng, F. Luo, and et al., "Reliability evaluation of distribution systems with mobile energy storage systems," *IET Renew. Power Gener.*, vol. 10, no. 10, pp. 1562–1569, Jul. 2016.

[20] G. Koeppel and G. Andersson, "Reliability modeling of multi-carrier energy systems," *Energy*, vol. 34, no. 3, pp. 235–244, Jun. 2009.
[21] K. Wang, H. Li, Y. Feng, and G. Tian, "Big data analytics for system stability evaluation strategy in the energy internet," *IEEE Trans. Industrial Informatics*, vol. 13, no. 4, pp. 1969–1978, Apr. 2017.
[22] M.-H. Shariatkhah, M.-R. Haghifam, M. Parsa-Moghaddam, and P. Siano, "Modeling the reliability of multi-carrier energy systems considering dynamic behavior of thermal loads," *Energy Build.*, vol. 103, pp. 375–383, Sep. 2015.
[23] M.-H. Shariatkhah, M.-R. Haghifam, G. Chicco, and M. Parsa-Moghaddam, "Adequacy modeling and evaluation of multi-carrier energy systems to supply energy services from different infrastructures," *Energy*, vol. 109, pp. 1095–1106, 2016.
[24] G. Li, Z. Bie, Y. Kou, and et al., "Reliability evaluation of integrated energy systems based on smart agent communication," *Appl. Energy*, vol. 167, pp. 397–406, 2016.
[25] Y. Lei, K. Hou, Y. Wang, and et al., "A new reliability assessment approach for integrated energy systems: Using hierarchical decoupling optimization framework and impact-increment based state enumeration method," *Appl. Energy*, vol. 210, pp. 1237–1250, 2018.
[26] X. Fu, Q. Guo, H. Sun, and et al., "Estimation of the failure probability of an integrated energy system based on the first order reliability method," *Energy*, vol. 134, pp. 1068–1078, 2017.
[27] X. Fu and X. Zhang, "Failure probability estimation of gas supply using the central moment method in an integrated energy system," *Appl. Energy*, vol. 219, pp. 1–10, 2018.
[28] M. D. Al-Falahi, S. Jayasinghe, and H. Enshaei, "A review on recent size optimization methodologies for stand-alone solar and wind hybrid renewable energy system," *Energy Convers. Manage.*, vol. 143, pp. 252–274, 2017.
[29] G. Zhang, B. Wu, A. Maleki, and W. Zhang, "Simulated annealing-chaotic search algorithm based optimization of reverse osmosis hybrid desalination system driven by wind and solar energies," *Solar Energy*, vol. 173, pp. 964–975, 2018.
[30] W. Zhang, A. Maleki, and M. A. Rosen, "A heuristic-based approach for optimizing a small independent solar and wind hybrid power scheme incorporating load forecasting," *J. Clean Prod.*, vol. 241, pp. 1–18, 2019.
[31] W. Zhang, A. Maleki, M. A. Rosen, and J. Liu, "Sizing a stand-alone solar-wind-hydrogen energy system using weather forecasting and a hybrid search optimization algorithm," *Energy Convers. Manage.*, vol. 180, pp. 609–621, 2019.
[32] A. Maleki, M. G. Khajeh, and M. Ameri, "Optimal sizing of a grid independent hybrid renewable energy system incorporating resource uncertainty, and load uncertainty," *Int. J. Electr. Power Energy Syst.*, vol. 83, pp. 514–524, 2016.
[33] C. Andalib-Bin-Karim, X. Liang, and H.-U. A. Chowdhury, "Generation reliability assessment of stand-alone hybrid power system-a case study," in *2017 IEEE International Conference on Industrial Technology (ICIT)*. IEEE, 2017, pp. 434–439.
[34] A. Rathore and N. Patidar, "Reliability assessment using probabilistic modelling of pumped storage hydro plant with pv-wind based standalone microgrid," *Int. J. Electr. Power Energy Syst.*, vol. 106, pp. 17–32, 2019.
[35] W. Wei and J. Wang, *Modeling and Optimization of Interdependent Energy Infrastructures*. Springer, Switzerland, 2020.
[36] P. M. Esfahani and D. Kuhn, "Data-driven distributionally robust optimization using the wasserstein metric: Performance guarantees and tractable reformulations," *Math. Program.*, vol. 171, no. 1-2, pp. 115–166, Sep. 2018.
[37] N. Fournier and A. Guillin, "On the rate of convergence in wasserstein distance of the empirical measure," *Probab. Theory Relat. Fields*, vol. 162, no. 3-4, pp. 707–738, Aug. 2015.
[38] W. Wei, F. Liu, and S. Mei, "Real-time dispatchability of bulk power systems with volatile renewable generations," *IEEE Trans. Sustain. Energy*, vol. 6, no. 3, pp. 738–747, Jul. 2015.
[39] G. A. Hanasusanto, V. Roitch, D. Kuhn, and W. Wiesemann, "A distributionally robust perspective on uncertainty quantification and chance constrained programming," *Math. Program.*, vol. 151, no. 1, pp. 35–62, 2015.
[40] R. Oberdieck, N. A. Diangelakis, M. Papathanasiou, and et al., "POP - parametric optimization toolbox," *Ind. Eng. Chem. Res.*, vol. 55, no. 33, pp. 8979–8991, Jul. 2016.
[41] D. Ke, C. Chung, and Y. Sun, "A novel probabilistic optimal power flow model with uncertain wind power generation described by customized Gaussian mixture model," *IEEE Trans. Sustain. Energy*, vol. 7, no. 1, pp. 200–212, Jan. 2016.
[42] M. Jia, C. Shen, and Z. Wang, "A distributed probabilistic modeling algorithm for the aggregated power forecast error of multiple newly built wind farms," *IEEE Trans. Sustain. Energy*, vol. 10, no. 4, pp. 1857–1866, Oct. 2019.

Yang Cao (S'18) received the B.Sc. degree in electrical engineering from Tsinghua University, Beijing, China, in 2017, where he is currently pursuing the Ph.D. degree.

His research interests include planning and operation of multi-carrier energy systems.

Wei Wei (M'15-SM'18) received the Bachelor and Ph.D. degrees both in electrical engineering from Tsinghua University, Beijing, China, in 2008 and 2013, respectively.

He was a Postdoctoral Researcher with Tsinghua University from 2013 to 2015. He was a Visiting Scholar with Cornell University, Ithaca, NY, USA, in 2014, and with Harvard University, Cambridge, MA, USA, in 2015. He is currently an Associate Professor with Tsinghua University. His research interests include applied optimization and energy system economics.

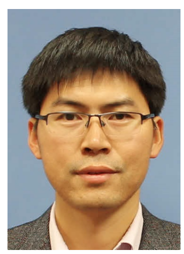

Laijun Chen (M'12) received the B.S. and Ph.D. degrees in electrical engineering from Tsinghua University, Beijing, China, in 2006 and 2011, respectively, where he is currently an Associate Professor.

His research interests include power system analysis and control, and renewable energy integration.

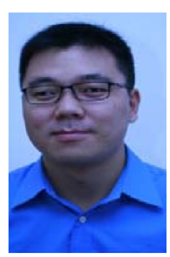

Qiuwei Wu (M'08-SM'15) received the Ph.D. degree in power system engineering from Nanyang Technological University, Singapore, in 2009. He was a Senior Research and Development Engineer with VESTAS Technology R&D Singapore Pte, Ltd., from March 2008 to October 2009. He has been an Assistant Professor with the Department of Electrical Engineering, Technical University of Denmark, Kongens Lyngby, Denmark, since 2009. In 2012, he was a Visiting Scholar with the Department of Industrial Engineering and Operations Research, University of California, Berkeley, for three months funded by Danish Agency for Science, Technology and Innovation, Denmark. He was a Visiting Scholar with the Harvard China Project, School of Engineering and Applied Sciences, Harvard University from 2017 to 2018.

His research interests include operation and control of power systems with high penetration of renewables, including wind power modeling and control, active distribution networks, and operation of integrated energy systems. He is the Deputy-Editor-in-Chief of the *International Journal of Electrical Power and Energy Systems*. He is an Editor of the *IEEE Transactions on Smart Grid* and *IEEE Power Engineering Letters*. He is the Regional Editor for Europe of the *IET Renewable Power Generation*, a Subject Editor of *IET Generation, Transmission and Distribution* and an Associate Editor of the *Journal of Modern Power Systems and Clean Energy*.

Shengwei Mei (F'15) received the B.Sc. degree in mathematics from Xinjiang University, Urumqi, China, the M.Sc. degree in operations research from Tsinghua University, Beijing, China, and the Ph.D. degree in automatic control from Chinese Academy of Sciences, Beijing, China, in 1984, 1989, and 1996, respectively.

He is currently a Professor of Tsinghua University, Beijing, China. His research interests include power system complexity and control, game theory and its application in power systems.